The distribution of ion orbit loss fluxes of ions and energy from the plasma edge across the last closed flux surface into the scrape-off layer

Weston M. Stacey and Matthew T. Schumann

Citation: Physics of Plasmas (1994-present) **22**, 042504 (2015); doi: 10.1063/1.4917318
View online: http://dx.doi.org/10.1063/1.4917318
View Table of Contents: http://scitation.aip.org/content/aip/journal/pop/22/4?ver=pdfcov
Published by the AIP Publishing

The distribution of ion orbit loss fluxes of ions and energy from the plasma edge across the last closed flux surface into the scrape-off layer

Weston M. Stacey and Matthew T. Schumann
Fusion Research Center, Georgia Institute of Technology, Atlanta, Georgia 30332, USA

(Received 30 January 2015; accepted 30 March 2015; published online 10 April 2015)

A more detailed calculation strategy for the evaluation of ion orbit loss of thermalized plasma ions in the edge of tokamaks is presented. In both this and previous papers, the direct loss of particles from internal flux surfaces is calculated from the conservation of canonical angular momentum, energy, and magnetic moment. The previous result that almost all of the ion energy and particle fluxes crossing the last closed flux surface are in the form of ion orbit fluxes is confirmed, and the new result that the distributions of these fluxes crossing the last closed flux surface into the scrape-off layer are very strongly peaked about the outboard midplane is demonstrated. Previous results of a preferential loss of counter current particles leading to a co-current intrinsic rotation peaking just inside of the last closed flux surface are confirmed. Various physical details are discussed. © *2015 AIP Publishing LLC*.
[http://dx.doi.org/10.1063/1.4917318]

I. INTRODUCTION

The need to take into account in plasma transport calculations that plasma ions on internal flux surfaces could access loss orbits that would allow them to free-stream out of the plasma has long been recognized (e.g., Refs. 1–9). Stacey *et al.*[10–14] have recently extended the Miyamoto[6] model for numerical calculations of the effects of these "ion orbit losses" (IOLs) on the interpretation of edge plasma transport, and deGrassie *et al.*,[15,16] Stacey *et al.*,[17,18] and Pan *et al.*[19,20] have shown that the peaking of toroidal rotation in the plasma edge observed in experiment could be interpreted as intrinsic rotation due to ion orbit loss.

The basic ion orbit loss calculation employed by these latter authors[10–20] consists of a solution of the Miyamoto canonical toroidal angular momentum, energy, and magnetic moment conservation equations to determine if an ion with a given direction and energy at a given location on an internal flux surface is "energetically" allowed to reach a point on or outside the last closed flux surface (LCFS). Different computational strategies are used by the three sets of authors to numerically combine multiple such basic IOL calculations to determine the loss of thermalized plasma ions and their energy and momentum from the edge plasma.

Our previous investigations[10–14] indicate that a very large fraction of the total ion particle and energy flux crossing the LCFS is carried by IOL ions. There are also indications that the poloidal distribution of the IOL particle and energy fluxes across the LCFS is very different than those of the particle and energy fluxes transported in the plasma. However, our previous IOL investigations used a computational strategy that emphasized the determination of the fraction of ions and energy that was ion orbit lost, but did not focus on where these IOL fluxes crossed the LCFS. The main purpose of this paper is to investigate the effect of ion orbit loss on the distribution over the last closed flux surface of the particle, energy, and momentum fluxes crossing from the confined plasma into the surrounding scrape-off layer (SOL). This investigation requires modifications of the computational strategy described in Refs. 10 and 13 with the objectives of calculating the poloidal distribution of ions, energy, and momentum from the edge plasma into the surrounding SOL. A secondary purpose is to investigate the possible effect on ion orbit loss of isotropization of the ion distribution by scattering.

II. CALCULATION MODEL

A. Basic ion orbit loss calculation

The basic ion orbit loss calculation considers an ion at a point with the poloidal angle θ_0 on an internal flux surface ψ_0 with the normalized minor radius ρ_0 and major radius R_0, which has a direction cosine of particle velocity with respect to the toroidal magnetic field ζ_0 and a speed V_0. The magnetic field ratio (toroidal/total) at this location is $f_{\varphi 0} \equiv |B_{\varphi 0}/B|$ and the electrostatic potential is ϕ_0. The equations for conservation of canonical toroidal angular momentum, energy, and magnetic momentum can be combined to obtain a quadratic equation[10] with terms evaluated at a point on the internal flux surface—subscript "0"—and at a point on the separatrix or last closed flux surface—subscript "s."

$$V_0^2\left[\left(\left|\frac{B}{B_0}\right|\frac{f_{\varphi 0}}{f_\varphi}\zeta_0\right)^2 - 1 + \left(1-\zeta_0^2\right)\left|\frac{B}{B_0}\right|\right] + V_0\left[\frac{2e(\psi_o-\psi)}{Rmf_\varphi}\left(\left|\frac{B}{B_0}\right|\frac{f_{\varphi 0}}{f_\varphi}\zeta_0\right)\right] + \left[\left(\frac{e(\psi_0-\psi)}{Rmf_\varphi}\right)^2 - \frac{2e(\phi_0-\phi)}{m}\right] = 0. \quad (1)$$

If this equation has a physical solution for a point on the LCFS ψ_s (or any other location) with normalized minor radius ρ_s, major radius R_s, poloidal angle θ_s, and magnetic field B_s, then that ion can be lost from the confined plasma through that point. In the GTEDGE code (a background modeling and experimental data interpretation code), this equation is solved many times for each of 8 values of θ_s, 8 values of θ_0, 22 values

of ζ_0 over $-1<\zeta_0<1$ (see Figure 1), and 24 values of ρ_0, using experimental radial electric field and ion temperature and using a constant current density approximation for the flux surface variable $\psi = RA_\varphi = \frac{1}{2}\left(\frac{\mu_0 I}{2\pi a^2}\right)\bar{R}r^2$ in order to generate the minimum physically realistic value of $E_{\min}(\zeta_0, \rho_0, \theta_0, \theta_s) = 1/2mV^2_{0\min}(\zeta_0, \rho_0, \theta_0, \theta_s)$ as input for the IOL numerical computational strategy. Here, A_φ is the vector potential and I is the plasma current. The effect of the constant current density approximation is presently being investigated.

B. IOL computation strategy—General considerations

At a certain radial location (designated ρ_1)in the plasma edge the outward flowing ion population, which is assumed to be uniformly distributed over the flux surface and in a Maxwellian distribution at the local (radial) ion temperature, the $E_{\min}(\zeta_0, \rho_0, \theta_0, \theta_s)$ is sufficiently low that a small fraction (<1%) of the ion distribution is at higher energy. The edge region between ρ_1 and the last close flux surface at ρ_s is divided into 24 equal-spaced intervals at normalized radii ρ_k for the purpose of calculating $E_{\min}(\zeta_0, \rho_0 = \rho_k, \theta_0, \theta_s)$, allowing the subsequent calculation of the fraction of the ions that would have flowed across each of these ρ_k surfaces in the absence of IOL that actually are ion orbit loss.

Since the ions follow the helical magnetic field lines around the flux surface many, many times in the time required to be transported outward from ρ_k to ρ_{k+1}, an ion reaching surface ρ_k at, e.g., $\theta_0 = 0$ and energy $E > E_{\min}(\zeta_0, \rho_0 = \rho_k, \theta_0 = 0, \theta_s)$ for some θ_s will be lost immediately, but an ion with $E < E_{\min}(\zeta_0, \rho_0 = \rho_k, \theta_0 = 0, \theta_s)$ will spiral to $\theta_0 = \pm\pi/4$, depending on the sign of ζ_0, and may be ion orbit lost from that location if $E > E_{\min}(\zeta_0, \rho_0 = \rho_k, \theta_0 = \pm\pi/4, \theta_s)$ for some θ_s, etc. Several strategies for sorting through such sequences of IOL possibilities are discussed below.

C. IOL computational strategy No. 1—"Original"

For each internal location θ_0 on each internal flux surface,[10] $E_{\min}(\zeta_0, \rho_0, \theta_0, \theta_s)$ is determined for all 8 exit locations θ_s on the LCFS and the smallest such energy is taken as the minimum loss energy for that $(\zeta_0, \theta_0, \rho_0)$, then the smallest such $E^{small}_{\min}(\zeta_0, \rho_0, \theta_0)$ or the average $E^{av}_{\min}(\zeta_0, \rho_0, \theta_0)$ over the 8 values of θ_0 is taken as the $E^{surf}_{\min}(\zeta_0, \rho_0)$ for the flux surface for that ζ_0. These last two procedures were found to yield similar results. This strategy is based on two assumptions: (i) that any ion on flux surface ρ_0 will spiral through all locations θ_0 in the time it takes to be transported across flux surface ρ_0; and (ii) that ions from any location θ_0 will be able to reach any energetically allowed location θ_s on the LCFS.

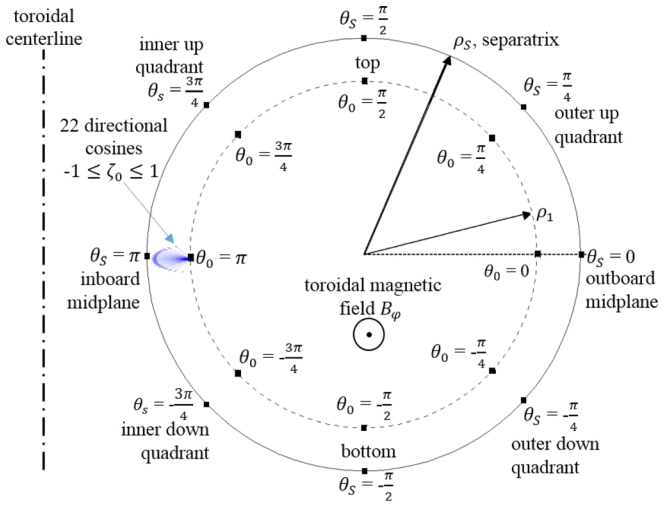

FIG. 1. Poloidal location schematic for basic ion orbit loss calculation.

D. IOL computational strategy No. 2—"New"

Strategy No. 1 was implemented in order to make a calculation of the loss fractions of ions, energy, and momentum, not to calculate the poloidal locations to which they were lost. Strategy number 2 has the calculation of poloidal loss locations of ions, energy, and momentum crossing the LCFS into the SOL as a major objective. To this end, we have modified the basic calculation describe above to calculate separate loss fractions from differential radial regions (instead of the cumulative calculations made for strategy 1) and to consider the allocation of those losses over the various energetically possible poloidal exit locations.

When it is energetically possible for an ion lost from a given location θ_0 on an internal flux surface at radial location ρ_0 to be lost through more that one exit location θ_s, we prorate the loss equally among all energetically possible loss locations. When it is not possible for an ion to be lost from location θ_0, we spiral the ion to the next nearest surface in the positive or negative direction in accordance with the sign of ζ_0, then check again if it can be lost.

E. IOL computational strategy No. 3—"Scatter"

This is strategy No. 2 plus the assumption that if the particle is not lost for the initial ζ_0 then the lowest $E_{\min}(\zeta_0, \rho_0, \theta_0)$ over the 22 values of ζ_0 will be used, because of the isotropization of the distribution by scattering.

F. Loss calculation

Once the minimum loss energy $E_{\min}(\zeta_0, \rho_0)$ for ions on internal surface ρ_0 with direction cosine ζ_0 is determined by one of the above computational strategies, the loss fraction that has taken place over $0 < \rho < \rho_0$ of the total ion population with directions cosine ζ_0 that would have been present in the absence of IOL can be calculated from

$$F_{loss}(\rho_0) = \frac{\int_{-1}^{1} d\zeta_0 \int_{V_0^{\min}(\rho_0,\zeta_0)}^{\infty} f(V_0) V_0^2 dV_0}{\int_{-1}^{1} d\zeta_0 \int_{0}^{\infty} f(V_0) V_0^2 dV_0} = \frac{\int_{-1}^{1} d\zeta_0 \int_{\varepsilon_{\min}(\rho_0,\zeta_0)}^{\infty} \varepsilon^{1/2} e^{-\varepsilon} d\varepsilon}{\int_{-1}^{1} d\zeta_0 \int_{0}^{\infty} \varepsilon^{1/2} e^{-\varepsilon} d\varepsilon} = \frac{\int_{-1}^{1} d\zeta_0 \Gamma\left(\frac{3}{2}, \varepsilon_{\min}(\rho_0, \zeta_0)\right)}{2\Gamma\left(\frac{3}{2}\right)}, \quad (2)$$

where $\varepsilon_{\min}(\rho_0,\zeta_0) \equiv E_{\min}(\rho_0,\zeta_0)/kT_{ion}(\rho_0)$, $\Gamma(3/2)$ is the complete gamma function of order 3/2, $\Gamma(n,a) = \Gamma(n) - \gamma(n,a)$, and $\gamma(n,a)$ is the incomplete gamma function of order n and argument a. These forms result from using the Maxwellian distribution. Similar derivations lead to the fractions of ion energy and momentum that are IOL lost from within surface ρ_0

$$E_{loss}(\rho_0) = \frac{\int_{-1}^{1} d\zeta_0 \Gamma\left(\frac{5}{2}, \varepsilon_{\min}(\rho_0,\zeta_0)\right)}{2\Gamma\left(\frac{5}{2}\right)},$$
$$\mathrm{M}_{loss}(\rho_0) = \frac{\int_{-1}^{1} d\zeta_0 \Gamma(2, \varepsilon_{\min}(\rho_0,\zeta_0))\zeta_0}{2\Gamma(2)}. \quad (3)$$

The fraction of ions lost by ion orbit loss within the volume between the flux surfaces at ρ_k and ρ_{k-1}, which is needed for the "new" calculation strategy No. 2, may be determined by subtraction $dF_{loss}(\rho_k) = F_{loss}(\rho_k) - F_{loss}(\rho_{k-1})$, similarly for dE_{loss} and dM_{loss}.

G. Treatment of energy spectrum

In order to facilitate numerical computation, the model described above is based on the implicit assumption that the thermalized plasma is in a Maxwellian distribution at the local ion temperature, but with those ions in each direction above the minimum loss energy for that direction missing. We note that there exist ion orbit loss models with a more detailed calculation of the energy spectrum of the remaining ions, but with much greater computation times (e.g., the particle following model of Chang *et al.*,[8] and the kinetic models of Stoltzfus-Dueck[21] and Seo *et al.*[22]

H. Definition of lost

The model presented in this and previous papers[10,13] can calculate whether or not an ion with a given energy and direction cosine located at a given location (ρ_0,θ_0) on an inner flux surface can reach a location (ρ_s,θ_s) at a different radial and poloidal location. In this and previous papers, we have chosen ρ_s to be on the LCFS and have used a factor $0 \le R_{loss}^{iol} \le 1$ to represent the probability that an ion from the interior reaching a point on the LCFS will leave the plasma and not return. It is of course possible to make other choices for (ρ_s,θ_s), e.g., the location of a limiter or divertor entrance. Calculation of the possibility that a particle that crosses the LCFS follows that orbit and returns into the plasma are under investigation.

III. APPLICATION TO A DIII-D H-MODE SHOT

The edge experimental profiles for DIII-D[23] shot #123302 at 2600 ms (R = 1.75 m, a = 0.885 m, κ = 1.84, I = 1.50 MA, $B_\varphi = -1.98$ T, $q_{95} = 3.86$ m, $P_{nb} = 8.66$ MW, $n_C/n_D = 0.03$) are shown in Fig. 2. The diverted DIII-D plasma is approximated as an equivalent circular plasma enclosing the same magnetic flux at the corresponding radius. Most of the model parameters depend on the values on

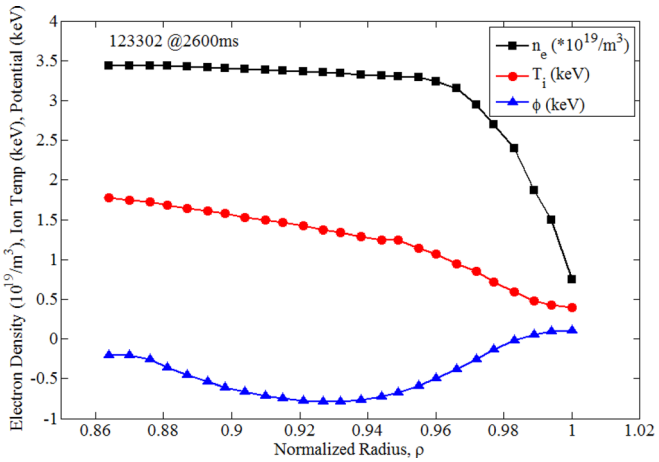

FIG. 2. Edge experimental density, temperature, and electrostatic potential profiles for a DIII-D H-mode shot.

the flux surface, not on the geometric location of the flux surfaces. The effect of this geometrical approximation and the neglect of the Shafranov shift are presently being investigated. The lowest values of the calculated $E_{\min}(\zeta_0,\rho_0)$ at any location θ_0 on several internal flux surfaces are shown in Fig. 3. The lower $E_{\min}(\zeta_0,\rho_0)$ for the counter-current ions at all radial locations is notable.

The minimum loss energy for the innermost flux surface at $\rho_0 = \rho_1 = 0.864$ is show in Fig. 4. As may be inferred from Fig. 4, ions at any poloidal location θ_0 on the internal flux surface with sufficient energy to be lost at $\theta_s = \pi$ have sufficient energy to be lost at any other exit location on the LCFS, those that have sufficient energy to be lost from $\theta_0 = \pm 3\pi/4$ have sufficient energy to be lost over 3/4 of the locations on the LCFS, etc. This situation is illustrated in Fig. 5. In the new computational strategy No. 2 ions which energetically could escape across multiple locations on the LCFS are prorated equally among these locations.

The cumulative loss fractions of ions and energy from ion orbit lost particles from inside of radius ρ, i.e., for $0 < \rho_0 \le \rho$, are shown in Fig. 6, for both the original

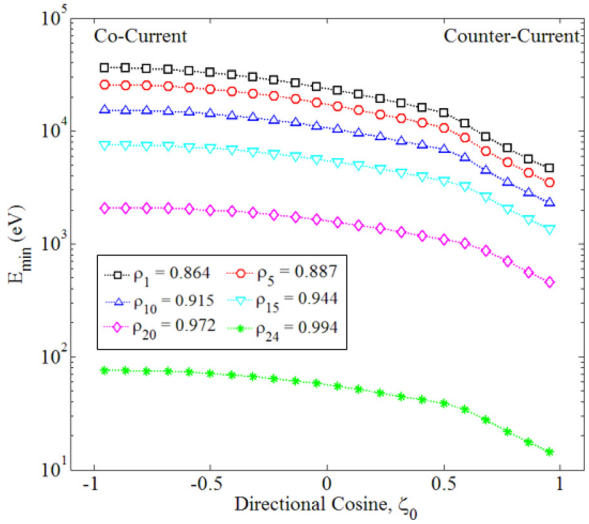

FIG. 3. Lowest value of $E_{\min}(\zeta_0,\rho_0)$ for any launch location θ_0 on several internal flux surfaces.

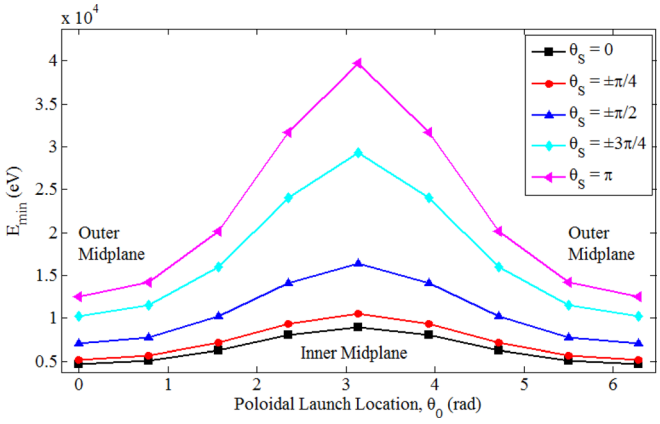

FIG. 4. $E_{\min}(\zeta_0 = 0.955, \rho_0 = 0.864, \theta_0, \theta_s)$ for counter-current ($\zeta_0 = 0.955$) ions launched at θ_0 on $\rho_0 = \rho_1 = 0.864$ to be lost at θ_s on the LCFS at $\rho_s = 1.0$.

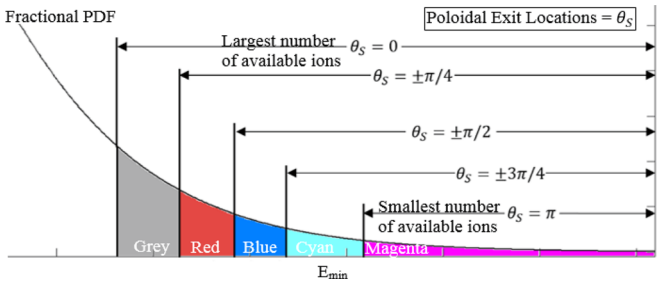

FIG. 5. Accessible poloidal exit locations as a function of ion energy.

computational strategy No. 1 used in previous papers and the new computational strategy No. 2 introduced in this paper. The new computational strategy No. 2 results in slightly larger loss fractions than the original computation strategy.

The poloidal distribution of the cumulative ion particle and energy ion orbit loss fractions across the LCFS calculated by the new computation strategies No. 2 and No. 3 (same as No. 2 but also including isotropization of the distribution in direction due to scattering) are shown in Fig. 7. The exiting distributions are strongly peaked about the outboard midplane at $\theta_s = 0$ for all three calculation strategies. This is consistent with a previous estimate[13] based on the

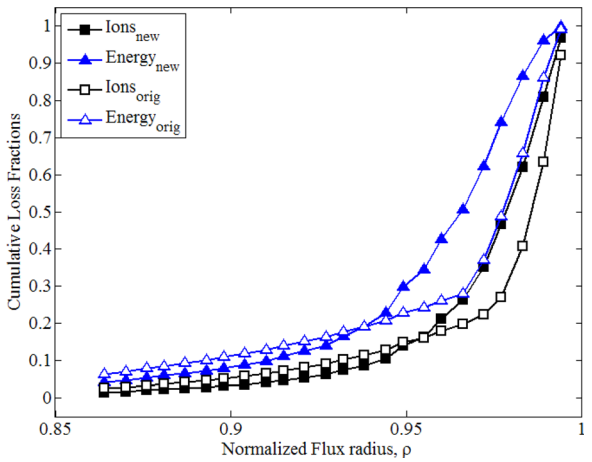

FIG. 6. Cumulative IOL ion and energy loss fraction at different radial flux locations.

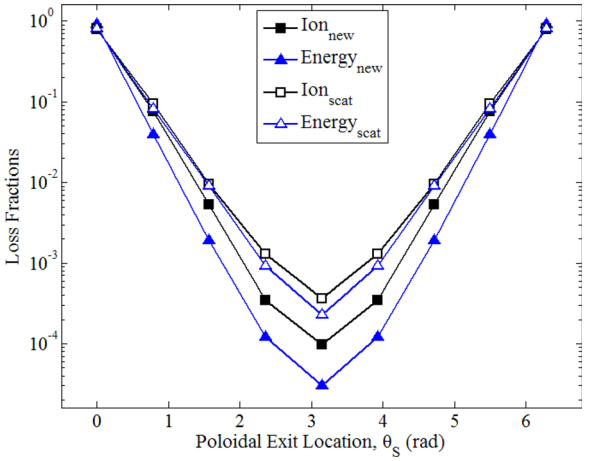

FIG. 7. IOL ion and energy loss fraction poloidal distribution over LCFS.

original calculation strategy No. 1 and with experimental data.[24–26] The isotropization assumption used to represent scattering in strategy No. 3 essentially assumes that all ions are scattered into the direction ζ_0 with the lowest value of $E_{\min}(\rho_0, \zeta_0)$, thus increasing greatly the calculated ion orbit loss fractions.

The poloidal distribution of particle and energy fluxes across the LCFS due to ion orbit loss are quite different than the distributions due to conductive or diffusive transport in the plasma, as shown in Fig. 8, where the normalized conductive energy flux calculated used an elongated plasma equilibrium (taking into account Shafranov shift and flux surface expansion and compression[27]) and the normalized IOL energy flux distribution corresponding to Fig. 7 are compared. Figure 6 indicates that more that 95% of the ion energy flowing across the LCFS is in the form of IOL ions and less that 5% is in the form of ion energy transported in the plasma.

We note, however, that some of the ions and energy that are IOL lost may return to the plasma if the loss orbit re-enters the plasma rather than striking the wall or a neutral particle. It should also be noted that we have not included

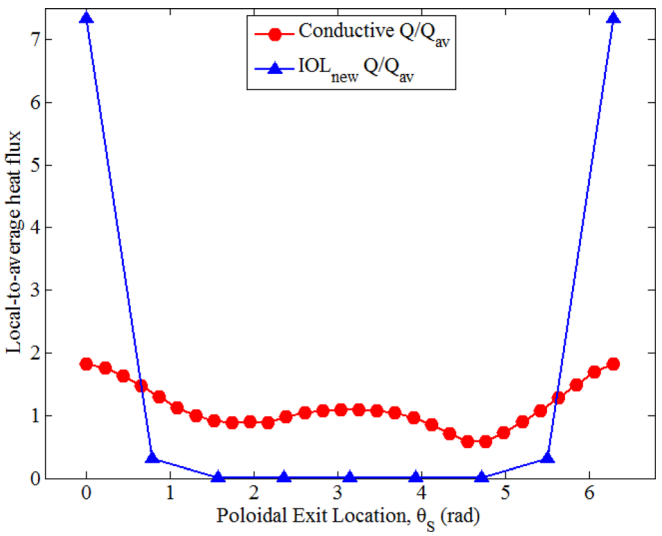

FIG. 8. Normalized poloidal energy flux distributions across LCFS due to conductive heat flux and ion orbit loss.

the X-loss of ions by grad-B and curvature drifting radially outward in the weak poloidal magnetic field region in the vicinity of the X-point,[8,28] which would be expected to cause a secondary peaking in the IOL distribution in Fig. 8 in the vicinity of the X-point at $\theta_s = 3\pi/2$.

The implications of Figs. 6 and 8 are quite interesting. The plasma ion and ion energy fluxes crossing the LCFS would consist of upwards of 90% IOL ions. If we assume that all the ions crossing the LCFS are lost and do not return inward across the LCFS into the plasma, then the fraction of the plasma energy transported outward by the ions (about half) will cross the LCFS near the outer mid-plane. The electron energy flux would be expected to cross the LCFS distributed more or less as the conductive flux in Fig. 8. If the energy split between ion and electron energy fluxes is roughly equal, then the ratio of energy flowing into the outer and inner SOLs, hence the outer and inner divertors, would be about 3/1. This is qualitatively consistent with experimental observation and should be testable quantitatively.

The preferential loss of counter-current ions leaves the edge plasma with a predominant co-current ion population, which can be calculated from[10]

$$\Delta V_{\|} = 2\pi^{-1/2} M_{loss}(\rho)\sqrt{2kT_{ion}(\rho)/m}. \quad (4)$$

This phenomenon causes an increasing with radius co-current toroidal rotation out to the radius slightly inside the LCFS at which the co-current ions have almost all been lost. Beyond this radius, the small loss of co-current ions begins to increase, reducing the predominance of co-current ions and thus producing the peaking in intrinsic rotation shown in Fig. 9. The results of three ion orbit loss calculations, corresponding to the three different calculation strategies discussed previously, are shown. We note that inclusion of isotropization (due to scattering) in the calculation not only increases the intrinsic rotation by an order of magnitude but also broadens and weakens the rather distinctive peaking seen in the two calculations without scattering and in experiments.[12,17–19] Our previous calculations and comparison with experiment of intrinsic rotation using the original calculation strategy No. 1 (subscript "orig" in Fig. 9) were in good agreement with respect to both the magnitude and the width of the intrinsic velocity peak, which causes us to doubt the full isotropization assumption that was used to calculate the much broader and order of magnitude larger result of assuming full isotropization shown with the subscript "scat" in Fig. 9.

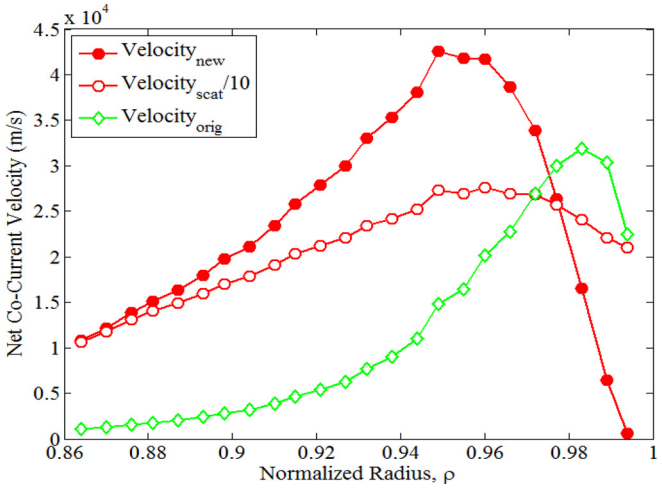

FIG. 9. Intrinsic co-current deuterium rotation (note that the rotation predicted with scattering isotropization is a factor of 10 larger than plotted).

IV. DISCUSSION

Our original modeling[10,13] of ion orbit loss has been extended to provide a better definition of the loss location distribution across the last closed flux surface. It is predicted that very large fractions of the particle and energy fluxes across the LCFS are in the form of IOL fluxes and that these IOL fluxes across the LCFS are very strongly peaked in the vicinity of the outboard mid-plane in a DIII-D H-mode discharge. This IOL flux distribution is very different than the predicted conductive/diffusive transport fluxes that are normally assumed to determine the distribution of exiting particle and energy fluxes in tokamaks. This has substantial implications for modeling and interpreting divertor physics in tokamaks (e.g., higher energy load to outboard divertor legs). One caveat is that the X-loss[8,28] of ions by grad-B and curvature drifts in the low-B_θ X-point region, which has not be treated in this paper, could produce a secondary peaking of IOL fluxes at the X-point.

The major heat removal problem for future tokamaks (e.g., ITER) is the heat flux from the outboard SOL into the outboard divertor. It would appear from the results of this paper that a major cause of this larger heat flux on the outboard than the inboard divertor is due to the ion orbit loss of energy (and particles) predominantly to the outboard scrape-off layer. This raises the possibility that alteration of this IOL distribution of particle and heat fluxes could ameliorate this heat removal problem.

Scattering would affect the IOL modeling by (i) altering the balance equations which are the basis for the ion orbit loss calculation and (ii) by isotropizing the directionality of the particle distribution (i.e., scattering particles with direction such that they are not lost into directions for which they can be lost). Dealing with the first effect would require the use of particle following codes,[8] which would greatly complicate the present calculation. However, isotropization can readily be incorporated into the present strategy, and we find that it greatly increases the fraction of particles and energy that are ion orbit lost from internal flux surfaces. We are inclined to neglect scattering, but the issue is not resolved.

Both our original ion orbit loss calculational strategy[10,13] and the new strategy presented in this paper and in more detail in Ref. 29 predict the preferential loss of counter-current directed ions, leaving the plasma with a predominantly co-current intrinsic rotation. The peaking in this rotation just inside the LCFS, which is seen experimentally,[12,17–20] is predicted to be caused by the ion orbit loss of counter-current ions from deeper inside the LCFS combined with the loss of co-current ions from flux surfaces just inside the LCFS. Isotropization due to scattering significantly increases the magnitude of and broadens this calculated peaking of intrinsic co-rotation beyond what has been

observed experimentally, which is an argument against including scattering in the ion orbit loss calculation. Clearly, it would be useful to have measured Deuterium rotation velocities against which to compare and refine the predictions of the two IOL calculational strategies in order to guide their further refinement.

The results of this paper extend, but are generally in agreement with, previous IOL results.

ACKNOWLEDGMENTS

The authors are grateful to T. M. Wilks and T. G. Collart for insightful discussions on the computation methodology.

[1]F. L. Hinton and M. Chu, Nucl. Fusion **25**, 345 (1985).
[2]K. C. Shaing and E. C. Crume, Phys. Rev. Lett. **63**, 2369 (1989).
[3]K. C. Shaing, E. C. Crume, and W. A. Houlberg, Phys. Fluids B **2**, 1492 (1990).
[4]K. C. Shaing, Phys. Fluids B **4**, 171 (1992).
[5]K. C. Shaing, Phys. Plasmas **9**, 1 (2002).
[6]K. Miyamoto, Nucl. Fusion **36**, 927 (1996).
[7]G. F. Matthews, G. Corrigan, S. K. Erents, W. Fundamenski, A. Kallenbach, T. Kurki-Suonio, S. Sipila, and J. Spence, JET Report EFDA-JET-CP(02)01-02 (2002).
[8]C. S. Chang *et al*., Phys. Plasmas **9**, 3884 (2002).
[9]K. G. McClemente and A. Thyagaraja, Phys. Plasmas **13**, 042503 (2006).
[10]W. M. Stacey, Phys. Plasmas **18**, 102504 (2011).
[11]W. M. Stacey, R. J. Groebner, and T. E. Evans, Nucl. Fusion **52**, 114020 (2012).
[12]W. M. Stacey, M.-H. Sayer, J.-P. Floyd, and R. J. Groebner, Phys. Plasmas **20**, 012509 (2013).
[13]W. M. Stacey, Nucl. Fusion **53**, 063011 (2013).
[14]J.-P. Floyd, W. M. Stacey, R. J. Groebner, and S. C. Mellard, Phys. Plasmas **22**, 022508 (2015).
[15]J. S. deGrassie, R. J. Groebner, K. H. Burrell, and W. M. Solomon, Nucl. Fusion **49**, 085020 (2009).
[16]J. S. deGrassie, S. H. Muller, and J. A. Bodeo, Nucl. Fusion **52**, 013010 (2012).
[17]W. M. Stacey, J. A. Boedo, T. E. Evans, B. A. Grierson, and R. J. Groebner, Phys. Plasmas **19**, 112503 (2012).
[18]W. M. Stacey and B. A. Grierson, Nucl. Fusion **54**, 073021 (2014).
[19]C. Pan, S. Wang, and J. Ou, Nucl. Fusion **54**, 103003 (2014).
[20]W. M. Stacey and C. Pan, "Correction of NF54, 103003 (2014)," Nucl. Fusion (unpublished).
[21]T. Stoltzfus-Dueck, Phys. Plasmas **19**, 055908 (2012).
[22]J. Seo *et al*., Phys. Plasmas **21**, 092501 (2014).
[23]J. Luxon, Nucl. Fusion **42**, 614 (2002).
[24]T. W. Petrie *et al*., J. Nucl. Mater. **313–316**, 834 (2003).
[25]T. W. Petrie *et al*., J. Nucl. Mater. **337–339**, 216 (2005).
[26]T. W. Petrie, J. G. Watkins, L. L. Lao, and P. B. Snyder, Nucl. Fusion **43**, 910 (2003).
[27]W. M. Stacey and C. Bae, Phys. Plasmas **16**, 082501 (2009).
[28]W. M. Stacey, Phys. Plasmas **18**, 122504 (2011).
[29]M. C. Schumann, "The effect of ion-orbit-loss on the distribution of ion, energy and momentum from the edge plasma into the scrape-off layer in tokamaks," M.S. thesis (Georgia Institute of Technology, 2015).